

The Influence of Fuel Properties on Particulate Number Emissions from a Direct Injection Spark Ignition Engine

Felix Leach¹, Richard Stone¹, Dave Richardson²

1. University of Oxford, 2 Powertrain Research, Jaguar Cars Ltd.

ABSTRACT

The use of direct injection spark ignition (DISI) engines for passenger cars has increased; providing greater specific performance and lower CO₂ emissions. DISI engines, however, produce more particulate matter (PM) emissions than Port Fuel Injected (PFI) engines. Forthcoming European exhaust emissions legislation is addressing concerns over health effects of PM emissions. Accordingly, research into PM emission formation has increased.

A model developed by Aikawa et al. (2010) for PFI engines correlated PM number emissions with the vapour pressure and the double bond equivalent (DBE) of the components of the fuel. However there was no independent control of these parameters. This study investigates a particulate emissions index for DISI engines.

A single-cylinder optical access Spray Guided DISI engine was used to develop a Particulate Matter Number emissions Index (PN index) – modified from the PM index using industry standard measurements – through the use of model and commercially available fuels.

Model fuels were designed using Raoult's law and UNIFAC such that the DBE and vapour pressure of the fuel mix could be varied.

Engine tests were conducted, independently varying the DBE and the vapour pressure of the fuel. PM number emissions were measured using a Cambustion DMS500, the results were analysed alongside observations of the fuel spray to investigate the PN index.

The PN index has also been used to evaluate emissions from two commercially available EN228 fuels. The results demonstrate that the trend of the PN index is followed both with model fuels and commercial gasolines.

INTRODUCTION

Gasoline Direct Injection (GDI) engines have become the preferred standard for gasoline light-duty vehicles in the worldwide market. Advantages of GDI engines over Port Fuel Injected (PFI) engines include greater specific output and lower CO₂ emissions. However, GDI engines emit more Particulate Matter (PM) than PFI engines [1]. Increasingly stringent EU emissions legislation has led to increased interest in Particulate emissions and concern that modern GDI engines will not meet future legislation unless they are optimised for reduced particulate emissions [2]. Historically, particulate matter emissions have been expressed as a mass that is collected on a filter paper, but these mass limits have become so small that it is very difficult to achieve repeatable results. The EU particulate matter limit (4.5 mg/km) corresponds to about 250 µg (allowing for dilution) on a filter that might weigh 100 mg. A balance is needed with a readability of 0.1 µg, and corrections even need to be made for buoyancy. The filters have to be weighed in a room with temperature and humidity control; even so, the permitted variation in humidity (from 37-53%) can lead to a change in mass of 7 µg; [3]. The number and size are also significant since the deposition efficiency in the respiratory system is greatest for small particles. So it is potentially the smaller particles that are the most harmful, so this is another reason for the introduction of legislation that limits the total number of particles that are emitted [4]. Forthcoming European emissions legislation, EU6 – effective 1 September 2014, mandates a particle limit of 6×10^{12} /km reducing to 6×10^{11} /km within 3 years [5].

It is not surprising that different fuels have different levels of particulate matter emissions, and it is almost inevitable that even a single engine will not always be tested with the same fuel. So when comparisons are made between tests using different fuels, then it would be useful to have a particulate matter index that enables a correction to be made based on the key fuel properties.

Aikawa et al. [6] conducted tests with a Port Fuel Injection (PFI) engine and developed a model linking fuel composition with PM emissions. It links PM emissions with the Vapour Pressure (VP) and Double Bond Equivalent (DBE) of the components in the fuel weighted by Mass Fraction (W_i):

$$I(VP, DBE) = \sum_{i=1}^n \left[\frac{DBE_i + 1}{VP_i} \right] W_{ti} \quad (1)$$

DBE is a measure of how unsaturated a hydrocarbon is, and can be easily calculated from:

$$DBE = \frac{2C - H - N + 2}{2} \quad (2)$$

Where C , H , and N are the number of Carbon, Hydrogen, and Nitrogen atoms respectively present in an organic compound. As an example, toluene (methyl benzene, $C_6H_5.CH_3$) has a DBE of 4 as the corresponding saturated compound would be heptane (C_7H_{16}), which has a DBE of 0.

Aikawa et al. [6] use a PM index that is of the same form as Equation 1, but there is insufficient compositional information of their fuels available in their paper for the PM index to be calculated independently. It should also be noted that Aikawa et al. evaluated the vapour pressure at a range of temperatures, and found that a temperature of 443 K gave the best correlation between particulate emissions and the PM Index. This is discussed later in Figure 9 of this paper. The vapour pressure was not a direct measurement, but came from an empirical relation between the normal boiling point of each component and its vapour pressure at 443 K. Aikawa et al. found a strong correlation between the PM index and measured particulate emissions (Figure 1).

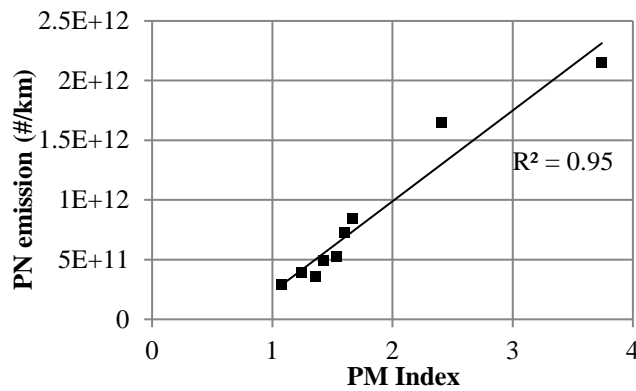


Figure 1: Relationship between PN (#/km) and PM index over NEDC (data from [6])

The work undertaken in [6] used a Port Fuel Injection (PFI) engine, and had no independent control of the fuel vapour pressure or DBE as commercial gasolines were used, along with a base fuel to which different components were added. Indolene was used as a base fuel, to which were added 10% by mass of components such as 2,2,4-Trimethylpentane, dodecane, ethylbenzene, and 1,2,4-trimethylbenzene. The PM index range of the fuels tested was 1.01 – 3.86 and the index range of over 1,400 worldwide fuels available was calculated and can be seen in Figure 2.

Figure 2 shows a very broad range of the PM Index of these worldwide fuels, with a mean of 2.12 and a standard deviation of 0.81.

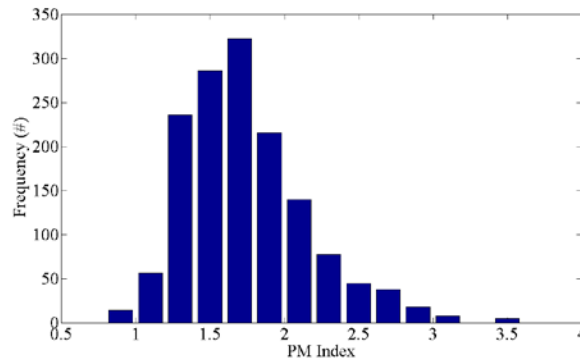


Figure 2: Range of PM indexes of a selection of commercially available fuels worldwide (data from [4])

The aim of this work is to review this index by independently controlling the volatility and double bond equivalent content of a fuel and extend the Particle Number (PN) measurements to a modern Spray Guided Direct Injection (SGDI) combustion system.

To avoid confusion in the current work the term PN Index is used here, with the vapour pressure being evaluated as Dry Vapour Pressure Equivalent (DVPE) with units of kPa and as a minor simplification the use of volume fraction (V_i):

$$\text{PN Index} = \frac{\sum_{i=1}^n [DBE_i + 1] V_i}{DVPE \text{ (kPa)}} \text{ (kPa}^{-1}\text{)} \quad (3)$$

EXPERIMENTAL METHODOLOGY

Engine

The engine for this work is a single-cylinder optical access Spray Guided Direct Injection (SGDI) engine supplied by Jaguar. The combustion system is essentially the same as that used in the Jaguar AJ133 engine, which has been comprehensively described by Sandford et al. [7]. SGDI engines are becoming very widely used in Europe, although for ease of manufacture some engines use a side mounted injector. A solid model view of the combustion system is shown in Figure 3.

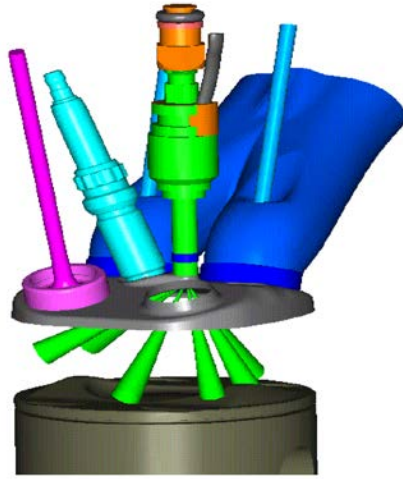


Figure 3: Solid model of the Jaguar AJ133 combustion system [7]

As shown in Figure 3, the injector delivers six spray plumes, four down into the cylinder and two plumes, which straddle the spark plug. The emission levels of SGDI type engines have the potential to meet the forthcoming particulate number emissions legislation, but as reported elsewhere the exact level would be very dependent on the warm-up strategy and any rich mixture excursions during accelerations [2].

Table 1 shows the engine specification and the valve timings. A lambda sensor was used to measure oxygen content in the exhaust and to set the correct fuel injection pulse width to achieve the mixture stoichiometry required for the test, for these tests, 10% rich. This was chosen because of the importance of slight rich mixture excursions on particulate emissions [8].

Table 1: Specifications of the single-cylinder optical access SGDI engine

Bore × Stroke	89 × 90.3 mm
Displacement	562 cm ³
Valves per Cylinder	2 intake, 2 exhaust
Compression Ratio	11.1
Fuel Pressure	150 bar
Injector	Bosch Multi-hole Nozzle
Valve Timing (°CA aTDC)	IVO 34°, IVC 242°, EVO 475°, EVC 5°

Instrumentation

Particulate emissions were measured using a Cambustion DMS500 Differential Mobility Spectrometer (DMS) [9]. This was used to provide both mass and number distributions, with the mass distributions being computed by Equation 4 [10].

$$Mass(\mu g) = 1.72 \times 10^{-15} d_p^{2.65} (nm) \quad (4)$$

Where d_p is the diameter of a particle in nm. This enables an estimate to be made of the mass that would be collected on a filter. A previous study [2] has shown that using the accumulation mode particle number from the DMS500 agrees very well with a Particle Measurement Programme (PMP) compliant solid particle counting system [3] that effectively discounts nucleation mode particles. In accordance with this, only the accumulation mode output was used. The correlation between DMS data and a legally compliant PMP test from earlier work can be seen in Figure 4 [11].

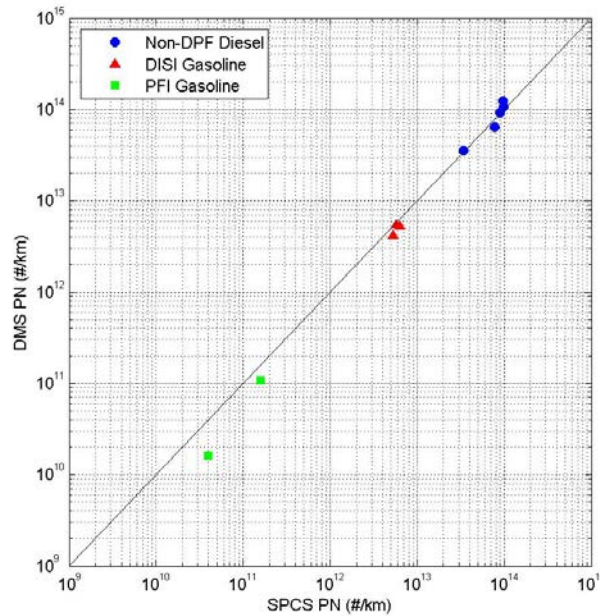


Figure 4: DMS500 PN result plotted against regulation-compliant SPCS PN result. For these data points, the DMS500 sampled directly from the vehicle tailpipe [11]

The engine was not fitted with a catalyst, and nor was hot air dilution of the exhaust gas used; both of these factors would lead to misleadingly high values of particulate matter emissions if the nucleation mode had been included. Hence only accumulation mode results have been used.

In-cylinder Hydrocarbon (HC) levels were measured using a Cambustion HFR400 fast Flame Ionization Detector (fFID), which measures hydrocarbon levels by chemi-ionization. Further details of the fFID are available in the literature [12]. For this experiment the hydrocarbon sample was taken at the circumference of the cylinder, approximately 10 mm below the cylinder head. Sampling in-cylinder with the fFID raises a number of issues compared with exhaust gas sampling. In particular due to large variations in cylinder pressure, large parts of the fFID signal are not valid due to back flow in the system, so fFID signals shown are for the valid parts of the signal – near top dead centre (tdc) on the compression stroke. The system had a response time of around 4 ms, which corresponds to 36°CA at 1500 rpm.

FUELS AND FUEL MODELLING

Evaporation modelling

The simplest model for evaporation uses the Raoult-Dalton law [13]. Raoult's law relates the vapour pressure of an ideal solution to the vapour pressure of each of its chemical components by the molar fraction of each component present.

$$y_i P = x_i P_{vpi} \quad (7)$$

Here y_i is the molar fraction of component i in vapour, x_i is the molar fraction of component i in liquid, P_{vpi} is the vapour pressure of component i , P is the pressure of the mixture.

Raoult's law requires there to be ideal mixing in the mixture, which gives Raoult's law its linear relationship. Ideal mixing is not the case for mixtures of aromatics and paraffins [14] so Raoult's law in isolation is not appropriate.

The UNIFAC extension to Raoult's Law [15] has been used to ensure that the components of the model fuels co-evaporate. The method is described in the Appendix.

UNIFAC provides temperature-dependent activity coefficients (γ_i), which modify Raoult's Law:

$$y_i P = \gamma_i x_i P_{vpi} \quad (8)$$

To validate this model, a distillation curve of a known fuel was modelled. The results in Figure 5 show that the UNIFAC model follows the distillation curve closely, with the exception of the beginning and end of the distillation, which can be attributed to distillation equipment artifacts.

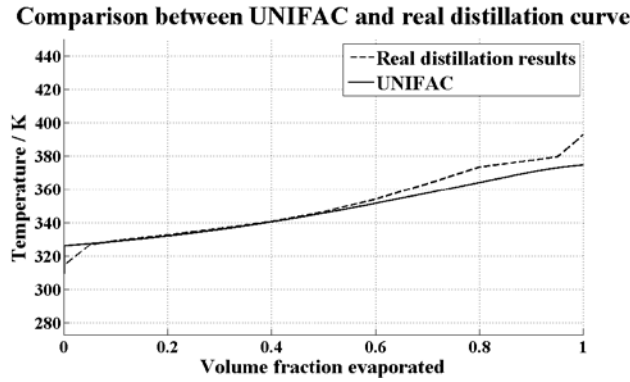


Figure 5: Comparison between UNIFAC model and real distillation of ULG

A sample of the results of the model is shown in Figure 6. These are plotted such that perfect coevaporation of aromatic and paraffin components is indicated by a straight line at unity on the ordinate. These results were used to set iso-octane : n-octane and iso-decane : n-decane ratios alongside the octane number which is discussed in the octane number considerations section.

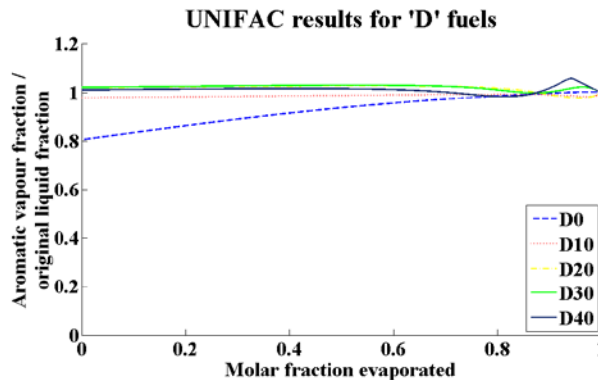


Figure 6: UNIFAC results on differing volatility fuels

Fuels

Our target was to vary the DBE and VP independently with model fuels, and to use unleaded gasolines with known properties; the model fuels were blended from pure components. The final composition for the model fuels is shown in Figure 7 and Table 2 (the 'T' and 'D' fuels). It can be seen that there is independent control over the double bond equivalent and vapour pressure of the fuel.

Toluene and 1,3,5-Trimethylbenzene were chosen as aromatic components having medium and high boiling points (both with a DBE of 4), and then their paraffin counterparts were selected on the basis of having adjacent boiling points, with blends selected to give co-evaporation with the corresponding aromatic component. Pentane was used to provide a volatile ‘front end’. When the volatility was varied, the aromatic content was kept at 35%, as it is the upper limit for the aromatic content in European gasoline and it maintains the octane number above 70.

Table 2: Test fuel composition

Fuel	Light components	Medium components			Heavy components			DBE+1	VP (kPa)	PM Index ³	PN Index
% v/v	n-pentane	iso-octane	n-octane	Toluene	iso-decane ¹	n-decane	TMB ²				
T0	5.00	71.25	23.75	0.00	0.00	0.00	0.00	1.00	15.79	0.341	6.33
T25	5.00	53.44	17.81	23.75	0.00	0.00	0.00	1.95	14.59	0.511	13.4
T35 ⁴	5.00	46.31	15.44	33.25	0.00	0.00	0.00	2.33	14.40	0.615	16.2
T50	5.00	35.63	11.88	47.5	0.00	0.00	0.00	2.90	13.66	0.762	21.2
T75	5.00	17.81	5.94	71.25	0.00	0.00	0.00	3.85	12.61	0.987	30.5
T100	5.00	0.00	0.00	95.00	0.00	0.00	0.00	4.80	11.73	1.19	40.9
D0 ⁴	5.00	46.31	15.44	33.25	0.00	0.00	0.00	2.33	14.40	0.615	16.2
D10	5.00	41.68	13.89	29.93	1.48	4.69	3.33	2.33	13.90	0.789	16.8
D20	5.00	37.05	12.35	26.60	2.96	9.37	6.65	2.33	13.38	0.962	17.4
D30	5.00	32.42	10.81	23.28	4.45	14.08	9.98	2.33	12.84	1.13	18.1
D40	5.00	27.79	9.26	19.95	5.93	18.77	13.30	2.33	12.27	1.31	19.0
D0*	0.00	48.75	16.25	35.00	0.00	0.00	0.00	2.40	8.55	0.408	28.1
D10*	0.00	43.88	14.63	31.50	1.56	4.94	3.50	2.40	7.87	0.541	30.5
D20*	0.00	39.00	13.00	28.00	3.12	9.88	7.00	2.40	7.22	0.674	33.2
D30*	0.00	34.13	11.38	24.50	4.68	14.82	10.50	2.40	6.52	0.806	36.8
D40*	0.00	29.25	9.75	21.00	6.24	19.76	14.00	2.40	5.79	0.937	41.5
Fuel 1	n/k	n/k	n/k	n/k	n/k	n/k	n/k	2.58	70.6	n/k	3.66
Fuel 2	n/k	n/k	n/k	n/k	n/k	n/k	n/k	2.25	88.6	n/k	2.54

1. 2,2,3,3-tetramethylhexane

2. 1,3,5-Trimethylbenzene

3. PM index calculated by %mass as in [6]

4. N.B. T35 \equiv D0

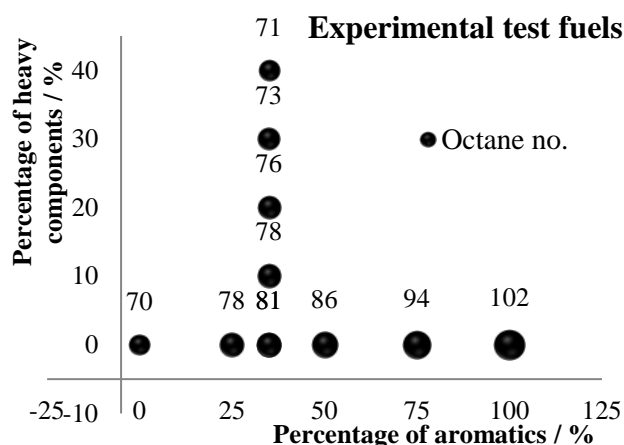


Figure 7: Research Octane Number (RON) of the model fuels with independent control of the aromatic content and volatility

The index was also tested against two fuels (Fuel 1 and Fuel 2) which meet pump gasoline specifications for summer fuels [16]. Their specification and distillation curves are shown in Table 2 and Figure 8.

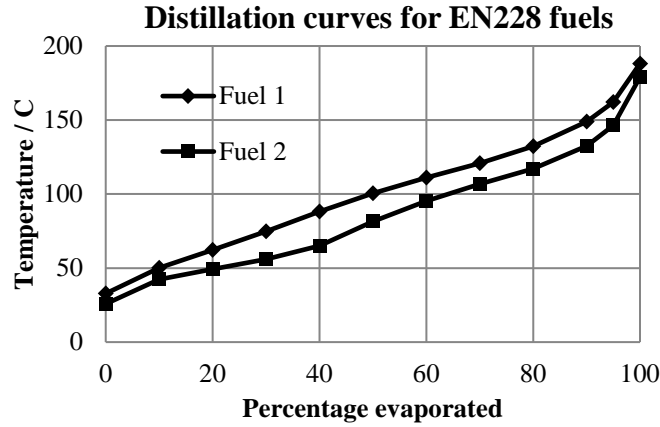


Figure 8: EN228 Fuel Distillation Curve

The incomplete compositional breakdown for the commercial fuels means that it is only possible to calculate the PN Index of these by their volume fractions, not their mass fractions. So unlike Aikawa et al. [6] the index has always been calculated here by volume fractions; an industry standard for fuel mixing. Comparisons with the model fuels indicate that for the majority of cases, the relative difference in calculation of the PM Index compared with the PN Index is less than 15%.

Vapour pressure of Gasoline is measured in accordance with EN 13016-1 [17] and an equivalent US standard and is expressed as Dry Vapour Pressure Equivalent (DVPE) or Reid Vapour Pressure (RVP). This standard uses a temperature of 37.8 °C (310.95 K), whereas the PM index in [6] uses Absolute Vapour Pressure at a temperature of 443 K. DVPE is intended to be equivalent to RVP [17], and is calculated from a statistical correlation equation to give a dry Reid Vapour Pressure. The differences between Reid Vapour Pressure, DVPE and Air Saturated Vapour Pressure (ASVP), are all small (and comparable to uncertainties when they are measured or modelled); they are all essentially absolute vapour pressures.

DVPE can easily be converted to ASVP from Equation 5 [18].

$$DVPE(kPa) = (0.965ASVP(kPa)) - 3.78 \quad (5)$$

The difference between ASVP and VP comes from the dissolved air in the liquid in the ASVP test. This can be approximated from Henry's Law (Equation 6 [18]).

$$p = k_h c \quad (6)$$

Here p is the partial pressure of the solute gas in solution, k_h is a temperature dependent coefficient, and c is the concentration of the solute.

k_h can be calculated from the Van't Hoff equations [18], and is temperature dependent. Henry's law can then be used to calculate the air dissolved in the liquid at 273.15 K that will come out of solution at 310.95 K. This will be an approximate conversion from VP to ASVP.

Aikawa et al [6] show that the correlation coefficient between the PM index and Particle Number emissions is still 0.90 for an Absolute Vapour Pressure calculation temperature of 310.95 K. This is shown in Figure 9.

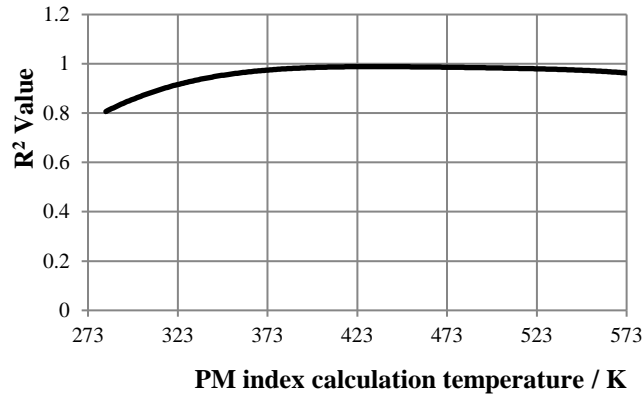


Figure 9: Fit of determination coefficient between Particle Number emissions and PM Index for different Vapour Pressure evaluation temperatures (data from [4])

For the model fuels mixed from pure components, for which the complete compositional breakdown was known, but DVPE was not known, the PN index was calculated using VP calculated at 310.95 K (using the UNIFAC method discussed in the Appendix) then converted to DVPE using the method discussed in this section. For commercial gasolines, the stated DVPE or RVP was used.

Octane number considerations

Ensuring mixture co-evaporation and homogeneity was a key goal throughout. This had to be balanced against the Research Octane Number (RON) of the fuel. Previous experiments have determined that at part load the minimum RON that this engine required was 70. This was a particular challenge as n-octane has a RON of -17; long straight-chain molecules coevaporate well with the aromatic components but have low RON values. The RON limit of 70 was key in choosing both the iso-octane : n-octane and iso-decane : n-decane ratios as well as setting the heavy component limit of 40%. It can be seen from Figure 7 that this criteria was met, and the ratios chosen are: iso-octane : n-octane ratio 75:25 and iso-decane : n-decane ratio 24:76.

RESULTS AND DISCUSSION

For these experiments the engine was run at a fixed operating point shown in Table 3. The engine was run with open loop Lambda control with a lambda of 0.9. This is to reflect the rich mixture excursions which are known to have a large effect on the particulate matter emissions [8].

Table 3: Engine operating point

IMEP (bar)	1.8
Inlet air temperature (°C)	40
Coolant temperature (°C)	60
Lambda	0.9
RPM	1500
Start of ignition (°CA bTDC)	35
Start of Injection (°CA bTDC)	280

Model fuels mixed from pure components

Figure 10 shows the PN emissions (in $\#/cm^3$) for the set of fuels with only light and medium components present, but varying aromatic content (and hence DBE). These test points are shown in Figure 7, with the octane number calculated for each fuel overlaid. It can be seen in Figure 10 that the Particulate Number emissions increase with the PN Index, but not linearly.

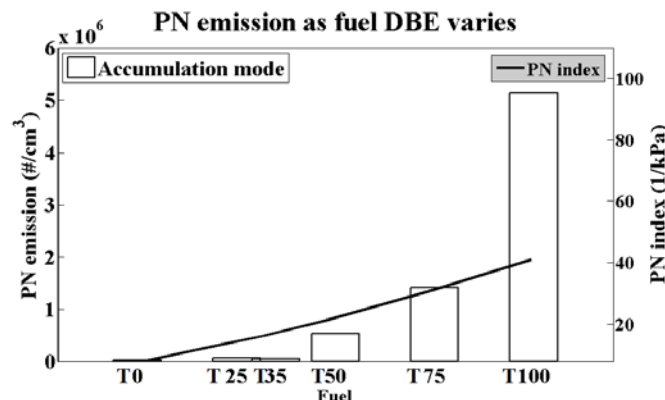


Figure 10: Accumulation mode Particulate Number emissions and PN Index dependence on the fuel aromatic content

Similarly Figure 11 shows the PN emissions (in #/cm³) for the set of fuels with constant DBE (in this case fixed by the 35% aromatic content, the upper level for EN228 ULG), but varying levels of decanes present (and hence vapour pressure). These test points are shown on Figure 7; overlaid on Figure 10, Figure 11, and Figure 14 is the PN index calculated for each fuel. It can be seen in Figure 10 and Figure 11 that the previously established trend of fuels with higher indices giving higher PN emissions is followed.

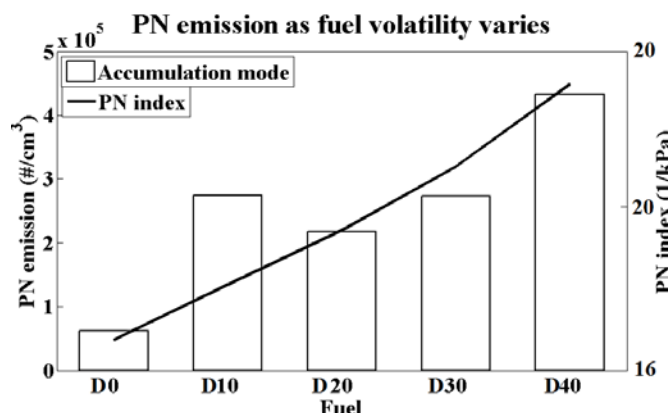


Figure 11: Accumulation mode Particulate Number emissions and PN Index value variation as the fuel Vapour Pressure is varied (fixed DBE)

Both Figure 10 and Figure 11 display rich ($\lambda = 0.9$) data. This gives clearer trends than with stoichiometric tests, and rich mixture excursions have been shown to be the source of the majority of the PN emissions over the NEDC [8]. These fuels have full independent control over VP and DBE and validate the trends shown in the PM Index [6].

The fuels used here all contain 5% n-pentane by volume, which is used to mimic the light end found in commercially available fuels. It can be shown that the presence of this light end is vital with fuels mixed from pure components in order that their evaporative performance, and hence PN emissions, are comparable with commercially available fuels.

Comparisons were run using identical fuels, with and without 5% n-pentane present. Figure 12 shows the evolution of the in-cylinder hydrocarbon levels, measured using a fFID, 10 mm below the cylinder head gasket on the cylinder liner. Measurements were taken over 69 runs, and at each crank angle the average and standard deviation were calculated. The standard deviation was used to give an indication of the cycle-to-cycle variations. It can be seen that the hydrocarbon levels are significantly higher, and rise faster, when there is pentane in the fuel, indicating more rapid dispersion of the fuel in the cylinder, and that the cycle-to-cycle variations are higher. This suggests that the mixture is less homogeneous when pentane is present, indicating that the presence of pentane leads to a breaking up of the spray sooner in the cylinder. Figure 13 shows that the effect of pentane on the peak fFID signal is the same, regardless of where around the cylinder liner that the hydrocarbon levels are sampled. However, the circumferential variations in the fFID signal are smaller when there is no pentane, and this (perhaps surprisingly) suggests that the pentane reduces the homogeneity of the mixture.

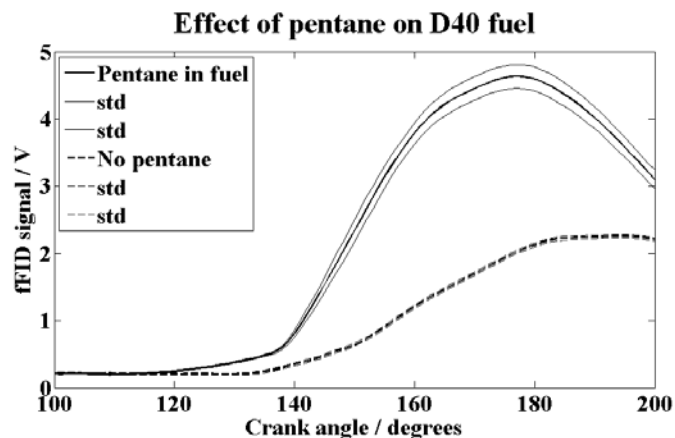


Figure 12: In-cylinder hydrocarbon levels sampled 10 mm below the cylinder head gasket and 120° around from the front of the engine

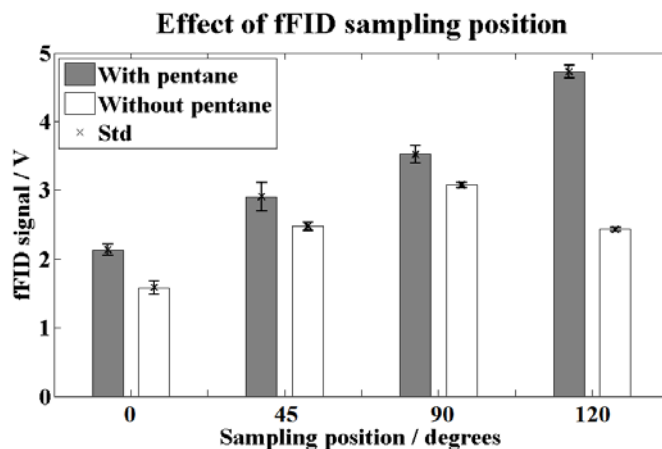


Figure 13: Effect of annular sampling position on the peak fFID signal for fuels with and without pentane; the standard deviation bars indicate the cycle-to-cycle variations in the mixture (0° is the front of the engine)

The effect of not adding pentane on the mixture homogeneity is also seen in the particulate emission results. Figure 14 shows the PN emissions (in $\#/\text{cm}^3$) for the set of fuels with a constant DBE (again fixed at a 35% aromatic content) but without 5% pentane added. Figure 14 shows that as the vapour pressure of the fuel is decreased (with fixed DBE), the level of the PN emissions also decreases, due to the increased mixture homogeneity. This trend is the opposite to that predicted by the PN Index, and shows the importance of adding high vapour pressure components, in small quantities, to make model fuels mixed from pure components more representative of commercial gasoline.

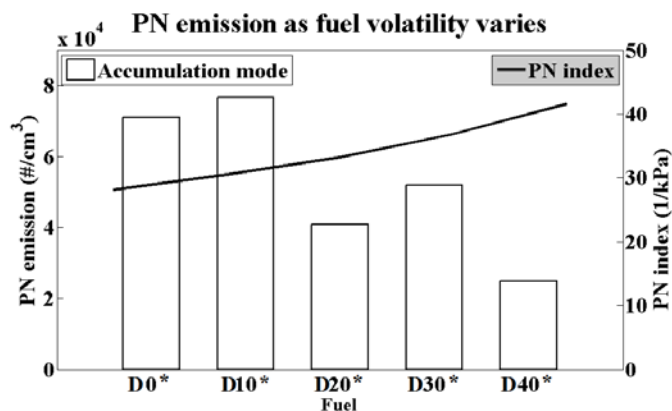


Figure 14: PN emissions as fuel Vapour Pressure is varied for fuels without pentane

Results with commercial fuels

Figure 15 shows the PN emissions (in $\#/cm^3$) for two fuels which meet EN228 as specified in Table 2. Again Figure 15 shows that the trends of the PN Index are reflected in the PN emissions of two fuels representative of commercially available gasoline. This is an important result as it shows that the index is applicable to commercially used fuels, when using a SGDI combustion system.

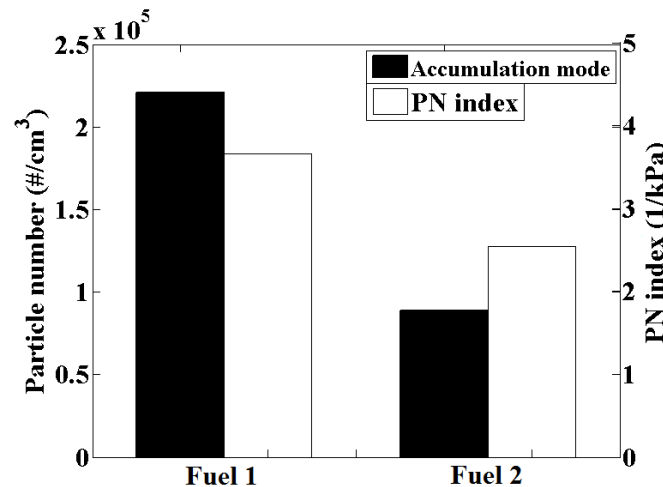


Figure 15: PN emissions from two fuels meeting EN228

SUMMARY/CONCLUSIONS

Particulate emissions from a SGDI engine have been studied experimentally using a Cambustion DMS500 Differential Mobility Spectrometer. Fuel blends have been designed that have independent control of the fuel volatility and aromatic content, and these have been used to validate a PN Index. It has been shown that to model fuel evaporation with mixtures of aromatics and paraffins, Raoult's Law needs to be extended by use of the UNIFAC method. This model can be used to ensure co-evaporation of aromatic and paraffin components in a model fuel, to avoid stratification of the individual components of a fuel in-cylinder. The effect of low boiling point components on the fuel spray is significant, and the addition of pentane to fuels mixed from pure components is important in order to reflect real world evaporation behaviour. This has been shown using both fast FID data, and particulate emissions data. Using these criteria, a recipe has been generated to create model fuels to mimic commercially available gasolines. A matrix of these model fuels has been tested on a single cylinder SGDI combustion system, and their PN emissions have been shown to follow the PN index. Two commercially available gasolines have also been tested on the same engine, again their PN emissions have been shown to follow the PN index. The PN index has been validated in a SGDI engine by using both model fuels and commercially available fuels. The PN Index has been shown to be an important parameter for fuel specification.

REFERENCES

- 1 Zhao, H. *Overview of Gasoline Direct Injection Engines*. In Zhao, H., ed. Advanced direct injection combustion engine technologies and development: Gasoline and gas engines (Woodhead Publishing Ltd and CRC Press, 2010).
- 2 Braisher, M., Stone, C.R. and Price, P. *Particle Number Emissions from a Range of European Vehicles*. SAE Technical Paper, 2010, 2010-01-0786.
- 3 Andersson, J., Giechaskiel, B., Muñoz-Bueno, R., Sandbach, E. and Dilara, P. *Particle Measurement Programme (PMP) Light-duty Inter-laboratory Correlation Exercise (ILCE_LD) Final Report*. (European Commission Joint Research Centre Institute for Environment and Sustainability, 2007).
- 4 Eastwood, P. *Particulate Emissions from Vehicles*. (SAE International and John Wiley & Sons, Ltd., 2008).
- 5 Commission Regulation 692/2008, OJ L 199 of 18.7.2008, p.130.
- 6 Aikawa, K., Sakurai, T. and Jetter, J.J. *Development of a Predictive Model for Gasoline Vehicle Particulate Matter Emissions*. SAE International Journal of Fuels and Lubricants, 2010, 3(2), 610-622.
- 7 Sandford, M., Page, G. and Crawford, P. *The All New AJV8*. SAE World Congress & Exhibition, April 2009 (SAE, Detroit, MI, USA, 2009).

- 8 Peckham, M.S., Finch, A., Campbell, B.W., Price, P. and Davies, M. *Study of Particle Number Emissions from a Turbocharged Gasoline Direct Injection (GDI) Engine Including Data from a Fast-Response Particle Size Spectrometer*. SAE 2011 World Congress & Exhibition, April 2011 (SAE, Detroit, MI, USA, 2011).
- 9 Reavell, K., Hands, T. and Collings, N. *A Fast Response Particulate Spectrometer for Combustion Aerosols*. SAE Powertrain & Fluid Systems Conference & Exhibition, October 2002 (SAE, San Diego, CA, USA, 2002).
- 10 Symonds, J.P.R., Price, P. and Stone, C.R. *Density of Particles Emitted from a Gasoline Direct Injection Engine*. European Aerosol Conference Thessaloniki, 2008).
- 11 Braisher, M. *Particulate Matter Emissions Measurements from Engines and Vehicles*. DPhil Thesis, Engineering Science (University of Oxford, Oxford, 2010).
- 12 Cheng, W.K., Summers, T. and Collings, N. *The fast-response flame ionization detector*. Progress in Energy and Combustion Science, 1998, 24(2), 89-124.
- 13 Reid, R.C., Prausnitz, J.M. and Poling, B.E. *The properties of gases and liquids*. (McGraw-Hill, New York ; London, 1987).
- 14 Vidal, J. *Thermodynamics: Applications in Chemical Engineering and the Petroleum Industry*. (Editions OPHRYS, 2003).
- 15 Fredenslund, A. and Gmehling, G. *Vapor-Liquid equilibrium using UNIFAC a group-contribution method*. (Elsevier North-Holland Inc., 1977).
- 16 EN228:2008 *Automotive fuels. Unleaded petrol. Requirements and test methods*. 2008).
- 17 EN 13016:2007. *Liquid petroleum products. Vapour pressure. Determination of air saturated vapour pressure (ASVP) and calculated dry vapour pressure equivalent (DVPE)*.
- 18 Atkins, P.W. *Physical Chemistry*. (Oxford University Press, 1994).
- 19 Abrams, D.S. and Prausnitz, J.M. *Statistical thermodynamics of liquid mixtures: A new expression for the excess Gibbs energy of partly or completely miscible systems*. AIChE Journal, 1975, 21(1), 116-128.
- 20 Poling, B.E., Reid, R.C., Prausnitz, J.M. and O'Connell, J.P. *The properties of gases and liquids*. (McGraw-Hill, New York ; London, 2001).

CONTACT INFORMATION

Richard Stone,
Dept of Engineering Science
University of Oxford
Parks Rd
Oxford
OX1 3PJ
UK

Richard.stone@eng.ox.ac.uk

ACKNOWLEDGMENTS

The authors would like to thank Roger Cracknell and Trevor Davies of Shell Global Solutions (UK) for their advice. The authors would also like to thank EPSRC and Jaguar Cars Ltd for funding this research.

APPENDIX

UNIFAC

The UNiversal Functional Activity Coefficient method (UNIFAC) was proposed by Fredenslund et al. [15], so as to extend Raoult's Law to account for non-ideal mixing. It combines the Analytical Solution of Groups (ASOG) method, relating activity coefficients to molecular structural group interactions, with the UNIQUAC (UNiversal QUAsiChemical) model [19]. It is a semi-empirical model to predict non-ideal mixture behaviour based on molecular size and known interactions. It breaks molecules into functional groups to model interactions using empirical data from experimentally determined interactions.

The model essentially breaks down into two parts: the combinatorial part, due to the differences in size and shape of the molecules; and the residual part, due to energy interactions.

The key equations are shown below [20]:

$$\begin{aligned}\ln \gamma_i &= \ln \gamma_i^C + \ln \gamma_i^R \\ \ln \gamma_i^C &= \ln \frac{\Phi_i}{x_i} + \frac{z}{2} q_i \ln \frac{\theta_i}{\Phi_i} + l_i - \frac{\Phi_i}{x_i} \sum x_j l_j \\ \ln \gamma_i^R &= \sum_k v_k^{(i)} (\ln \Gamma_k - \Gamma_k^{(i)}) \\ l_i &= \frac{z}{2} (r_i - q_i) - (r_i - 1) \\ z &= 10 \\ \theta_i &= \frac{q_i x_i}{\sum_j q_j x_j} \\ \Phi_i &= \frac{r_i x_i}{\sum_j r_j x_j}\end{aligned}$$

x_i is the molar fraction of component i

θ_i is the area fraction

Φ_i is the segment fraction

r_i is the molecular Van der Waals volume

q_i is the molecular surface area

Γ_k is the group residual activity coefficient and $\Gamma_k^{(i)}$ is the same in a solution only of molecules of type i